Propane Liquefaction with an Active Magnetic Regenerative Liquefier

John Barclay[1], Kriston Brooks[2], Jun Cui[2,3], Jamelyn Holladay[2], Kerry Meinhardt[2], Evgueni Polikarpov[2], and Edwin Thomsen[2]

1) *Emerald Energy NW, LLC. (EENW), Bothell, WA 98012*
2) *Pacific Northwest National laboratory (PNNL), Richland, WA 99254*
3) *Ames National Laboratory, Iowa State University, Ames, IA 50010*

Abstract

Magnetic refrigeration is a well-known cooling technique based on the magnetocaloric effect (MCE) of certain solids as they enter or leave a high magnetic field. An active magnetic regenerator (AMR) uses certain ferromagnetic materials simultaneously as MCE refrigerants and as a regenerator. An effective active magnetic regenerative refrigeration cycle consists of four steps: adiabatic magnetization with no heat transfer gas flow; heat transfer gas flow at constant high field; demagnetization with no heat transfer gas flow; and heat transfer gas flow at constant low field. The first heat transfer gas flow step from a cold-to-hot temperature in this cycle rejects heat from the magnetized regenerator to a hot sink and the second reverse heat transfer gas flow step from a hot-to-cold temperature absorbs heat from a cold source. One important application of this AMRR cycle is a very efficient cryogenic liquefier (AMRL). Our primary objectives of the present work are to characterize an AMRL liquefier, identify effective cooling power of the cold heat transfer gas from a single-refrigerant, reciprocating, dual magnetic refrigerator with intermittent cooling of the AMRR cycle with continuous process gas liquefaction and continuous parasitic heat leaks. For experiments in this work an AMRR with Gd refrigerant with ~3 T magnetic field changes in a 0.25 Hz cycle to liquefy pure propane gas at two different supply pressures. The measured rate of liquefaction and the elapsed time for each case were measured and used to determine the volume of propane collected and the cooling power of the AMRR at the liquefaction temperatures. These cooling power results were compared to the cooling power results obtained from the cool-down temperature vs. time data. The agreement between the two independent cooling power results was excellent after the duty cycle of each cooling process was properly treated.

Key words: propane; liquefaction; active-magnetic-regenerator; load-curve; coil-fin-tube-heat-exchanger; Gd

Corresponding author: John Barclay; johnbarclay@emeraldenergynw.com; 17505 7th Ave W; Bothell, WA 98012

Color in figures: Those figures in color in the article will be easier for readers to understand but can be changed to black and white if required.

Declaration of interest: John Barclay is a technical consultant for the Magnetic Liquefier Project at PNNL

Submission declaration: This article has not been submitted for publication elsewhere. The successful liquefaction of propane has been mentioned as an accomplishment in a DOE/EERE/FCTO Annual Merit Review presentation on the Magnetocaloric Hydrogen Liquefaction project by Dr. Jamie Holladay.

Introduction

While magnetic refrigeration has long been used for refrigeration well below 1 K in research laboratories, use of the technology for refrigeration above 1 K is more recent. In 1966, van Geuns [1] provided the first study of magnetic refrigeration for use between ~4 K and ~20 K using paramagnetic refrigerants where the total entropy of a refrigerant is largely magnetic entropy easily changed by variable applied magnetic induction. Using magnetic refrigeration for liquefaction was initially focused on helium with magnetic Carnot cycles below 20 K. Hakuraku and Ogata[2] produced superfluid helium at 1.8 K with a rotating paramagnetic refrigerant in thermal contact with liquid helium as it is magnetized near 4.2 K to reject heat into boiling helium. Upon thermal isolation from the heat sink, the MCE cooled the refrigerant by gradual demagnetization until the refrigerant reached ~1.8 K just before making thermal contact with a separate bath of liquid helium that was cooled to ~1.8 K as demagnetization was completed. Nakagome et al. and Numazawa et al. also used a Carnot-cycle magnetic refrigerator[3, 4] to re-condense helium gas at 0.1013 MPa and 4.2 K by controlled-demagnetization of paramagnetic gadolinium gallium garnet from high magnetic field to approximately zero magnetic field. This very low-temperature liquefier was improved by using dysprosium gallium-iron garnet with a larger MCE for a given field change and temperature cycle.

However, to increase temperature spans required to liquefy cryogens with bubble-point temperatures above ~20 K, recuperative or regenerative magnetic cycles were necessary to exploit the MCE. Prototypes based on recuperative cycles were demonstrated by Brown in 1976[5] and Steyert, Jr. in 1978[6]. A major advance was enabled by the invention of the active magnetic regenerator by Barclay and Steyert, Jr. in 1982[7] wherein the regenerator function of a regenerative refrigeration cycle was combined with the active refrigerant function for the cycle. Early analytical models[8] to the calculate performance of devices based on active magnetic regenerative refrigeration (AMRR) cycles predicted active magnetic regenerative liquefiers (AMRLs) have potential to substantially increase liquefier efficiency and thereby reduce measured work required to liquefy cryogens such as liquid hydrogen or liquid natural gas. Several groups have worked on hydrogen liquefaction using active magnetic regenerative refrigerators using liquid nitrogen at 77 K as the heat sink. The Thermo-Magnetic Group at Astronautics Corporation of America developed an AMRR design with dual, two-stage fixed regenerators and moving high-field superconducting magnets operating between 77 K and 20 K. This device used LN_2 as a heat sink for the AMRRs operating from 77 K to 20 K and simultaneously to pre-cool the gaseous hydrogen process stream to 77 K[9]. This detailed design, guided by extensive design calculations, component tests, and numerical modeling, incorporated two layers of ferromagnetic intermetallic-compound refrigerants GdPd and $GdNi_2$ and numerous innovative features. This device was the first application of bypass flow of cold helium heat transfer gas to augment liquefaction. The projected AMRR-stage efficiency was over 50% of ideal. Unfortunately, this innovative hydrogen AMRL prototype was never built and tested. Barclay and Brook analyzed and disclosed an AMRL design to span from room temperature to 20 K using numerous optimized AMRR stages coupled in series with helium as regenerator heat transfer gas and as cold bypass gas at each stage to step-wise cool and liquefy a hydrogen process stream[10]. Other experimental work on AMRLs with bypass flow for hydrogen liquefaction was done at Prometheus Energy[11]. Multi-material AMRRs without bypass flow were developed by A. Rowe et al. at the University of Victoria[12,13,14] and by R. Chahine et al. at University of Quebec at Three Rivers.[15]

Utaki et al.[16] analyzed three different combinations of conceptual AMRR-based liquefier designs combined in series with different heat exchange fluids but without bypass flow of heat transfer gas for liquefaction of hydrogen. They considered liquefaction with 8 stages of AMRRs rejecting heat into air at 300 K plus use of a Carnot magnetic refrigerator (CMR) stage for hydrogen condensation near 20 K. This group also considered a 5-stage AMRR with LNG as a heat sink at ~120 K plus a CMR stage at 20 K; and a 3-stage AMRR with LN_2 as a heat sink at ~77 K plus a CMR stage at 20 K to produce LH_2. This analytical thermodynamic modeling[17] work led

to several years of experimental development by Numazawa et al. on design, fabrication, and testing of reciprocating-regenerator AMRL prototypes without bypass gas to operate between 77 K and 20 K for liquefaction of hydrogen using LN_2 as the heat sink and for pre-cooling the gaseous hydrogen process stream[18].

Simultaneously with the Japanese group's effort, Jeong et al. in Korea also numerically analyzed, designed, built, and tested several two-stage AMRL prototypes for liquefaction of hydrogen with LN_2 for pre-cooling and the heat sink[19]. This group used fixed magnetic regenerators within fixed superconducting magnets that were charged and discharged rather than a configuration with reciprocating regenerators and fixed magnet or a fixed magnet with reciprocating regenerators. In a recent report[20] this group's test results using multi-layer magnetic regenerators with four different rare-earth intermetallic refrigerants are described.

The design complexities of highly-efficient cryogenic active magnetic regenerators have become very evident from differences between experimental results of lab-scale prototypes and predicted performance from various numerical models of associated designs[21,22].

One observation from these previous efforts is that to achieve a very high figure of merit (FOM) for liquefaction of cryogens, it is necessary to eliminate inefficient conventional gas stages such as those to produce LN_2 for pre-cooling of hydrogen or helium process streams in conventional Claude-cycle LH_2 and Collins-cycle LHe liquefiers. This lesson established a requirement that highly efficient multi-stage AMRR designs must have their hot heat sink near room-temperature[23]. It was therefore easy to appreciate one key objective of the magnetocaloric hydrogen liquefaction project at Pacific Northwest National Laboratory (PNNL)[24] was development of efficient magnetic liquefiers starting at near room temperature. Over the past few years several variations of an AMRR prototype with starting temperature of ~280 K have been analyzed, designed, built, and tested to better understand how AMRs work in comparison to predicted performance. This work has helped understand AMRR optimization for high FOM and the important relationship between specific cooling power of magnetic refrigerant and flows of heat transfer gas through ferromagnetic regenerators during the hot-to-cold blow steps of the AMR cycle[25]. In addition, this work has helped understand the effect of intermittent cooling of reciprocating dual regenerators during a complete AMR cycle on the average measured cooling power with continuous input of parasitic heat leaks and cooling/liquefaction of a process gas.

The present work reports on the liquefaction of propane with helium heat transfer gas entering the hot-to-cold blow at a fixed hot heat-sink temperature of ~280-285 K that was undertaken to design, build, and test a simple propane liquefier using an AMRR to help understand its operational interrelationships. For the same experimental conditions this reciprocating dual regenerator AMRR was previously characterized by measuring the cooling power vs. cold temperature using a high-surface area electrical resistance heater located between the dual magnetic regenerators in the cold heat exchanger. However, the direct cooling and liquefaction of a process gas such as propane with precisely known feed initial gas temperature, pressure, and mass flow rate and final equilibrium liquid propane temperature, pressure and liquid produced gives an independent measurement of the cooling power in liquefier mode. This paper describes results of successful experiments to liquefy propane at two different pressures using a reciprocating AMRR with dual ferromagnetic Gd regenerators, [26,27] that cools from ~285 K to ~218 K with only parasitic heat leak. Analysis of results from these experiments provides an understanding of intermittent vs. continuous cooling in an AMRR that is necessary to design process heat exchangers and heat transfer gas flow controls for more complex AMRLs that efficiently span from ~280 K to ~120 K for LNG, or from ~280 K to ~20 K for LH_2. No prior report of propane liquefaction with an AMRR has been published to our knowledge.

Ideal Specific Work for Liquefaction

The FOM is defined as the ratio of ideal work for liquefaction to real work for liquefaction for the same amount of gas under the same conditions. The real specific work (total work input per mass of cryogen produced) is a

measured quantity of an operating liquefier. The ideal specific work for a given set of initial conditions can be calculated assuming that the gas to be liquefied is ideally isothermally compressed from its initial starting pressure at near room temperature to a pressure high enough such that an ideal isentropic expansion of the compressed gas from that pressure will reach the bubble-point temperature of the cryogenic liquefied gas[28]. This ideal specific work is the minimum energy that must be expended to liquefy a unit mass of the gas. It differs for each gas and for different initial and final conditions of the liquefaction process. It can be calculated with the following equation:

$$\frac{\dot{W}}{\dot{m}} = T_H\left(S_H - S_{liq}\right) - \left(h_H - h_{liq}\right)$$

where $\dot{W}$ and $\dot{m}$ are the work rate and mass flow rate, respectively, and T_H, S_H, and h_H are the initial (hot) temperature, entropy, and enthalpy at the initial pressure of the gas to be liquefied. S_{liq} and h_{liq} are the entropy and enthalpy of the cryogenic liquid at its final conditions. The entropy and enthalpy values of different gases under different conditions as required can be calculated with real gas equations of state such as the Benedict, Webb, and Rubin equation used in the NIST code, Refprops. For example, at an initial temperature of 295 K and a pressure of 14.695 psia (0.1013 MPa), pure propane liquefies at 231.0 K with an ideal specific work as 130.1 kJ/kg.

Active Magnetic Regenerative Refrigeration Cycle

In a magnetic refrigeration cycle with a solid working refrigerant instead of a gas refrigerant, the relatively small ΔT_S vs. T data (see Fig. 1) show that to create a magnetic refrigerator that spans more than a few tens of Kelvin, a recuperative or regenerative magnetic cycle is required. The magnetic Brayton cycle has two constant magnetic field and two constant entropy steps which can be a very effective magnetic regenerative cycle. A ferromagnetic refrigerant near its magnetic ordering (Curie) temperature executes this cycle when it is heated by adiabatic magnetization with no heat transfer fluid flow, cooled by flow of a cold-to-hot heat transfer fluid at constant magnetic field, cooled by adiabatic demagnetization with no heat transfer fluid flow, and warmed by flow of a heat transfer fluid in the opposite direction to the first flow at constant magnetic field. Axial elements of magnetic refrigerant(s) comprising a compact, porous, high-performance cylindrical regenerator execute slightly different magnetic Brayton cycles that are thermally coupled together with periodic, reciprocately flows of heat transfer gas to create an active magnetic regenerator[29] (AMR) capable of pumping heat from a desired cold thermal load to a heat sink at a fixed hot temperature. Using an AMR with several layers of different magnetic refrigerants with sequentially different Curie temperatures, creates an active magnetic regenerative refrigerator (AMRR) that can span many times the ΔT_S of individual refrigerants. The active magnetic regenerative cycle is a unique cycle that does not have any direct analogy in gas-cycle refrigeration. This cycle enables innovative designs of AMRRs configured as very efficient liquefiers (AMRLs) for different gases such as propane, ethane, methane/natural gas, argon, nitrogen, oxygen, hydrogen, and helium that all liquefy below room temperature.

The cooling power of an AMRR is driven by the magnetocaloric effect of the magnetic refrigerants in regenerators. However, this cooling power is only achieved by optimum flow of heat transfer fluid through the magnetic regenerators at two constant magnetic field steps in the AMR cycle. Quantitatively, with an optimum hot-to-cold flow rate of helium heat transfer gas through the demagnetized regenerator, the cooling power of this regenerator, which occurs once every four steps of an AMR cycle, is given by

$$\dot{Q}_C(T_{COLD}) = \nu Fr_{COLD} M_S C_P(T_{COLD}, B_{\mathrm{Low}}) \Delta T_{CD}(T_{COLD}).$$

In this equation $\dot{Q}_C(T_{COLD})$ is the cooling power in W, ν is the AMR cycle frequency in Hz, Fr_{COLD} relates to the fraction of the regenerator length colder than the steady-state cold temperature T_{COLD} of the regenerator and it also includes the integral of the changing cold helium gas temperature vs time over the flow period. This

parameter depends upon the non-linear temperature profile of the magnetic solid in the flow direction of the regenerator, the total thermal load on the regenerator, and on the flow rate of heat transfer gas, M_S is the regenerator mass of the refrigerant in kg, C_P is the total heat capacity of the refrigerant at T_{COLD} and magnetic field after demagnetization in J/kg K, and ΔT_{CD} is the adiabatic temperature change upon demagnetization. All the variables in this equation are known except Fr_{COLD}. For different regenerators this parameter can be calculated for various AMR operating conditions by using the detailed 1-D numerical model for the dual Gd regenerators and other parameters used in this experiment[30]; typical values are ~0.2 to ~0.4. Assuming a process gas requires continuous cooling, it means 4 identical regenerators must be used in a reciprocating design. In the AMRR used for this experiment there are two identical regenerators as shown below.

Magnetocaloric properties of Gd

The magnetocaloric effect of a magnetic refrigerant is characterized by the isothermal entropy change and adiabatic temperature change as a function of temperature and magnetic induction or magnetic field[31]. The cooling power equation shows that analysis of experimental results such as cooling power requires precise values of the adiabatic temperature changes and total heat capacity. These properties at specific conditions are usually obtained from simulated values using the validated molecular mean field theory equation of state with the Debye model for lattice heat capacity and free-electron model for electronic heat capacity using measured Curie temperature, magnetic moment, Debye temperature, and other known physical properties. For example, the calculated adiabatic temperature change (ΔT_S) of ferromagnetic Gd as a function of temperature between discrete applied magnetic induction of 0.6 T and 3.3 T is shown below in Figure 1. These data agree very well with the experimental results[32]. Due to the reversibility of the magnetocaloric effect, the peak adiabatic temperature upon magnetization (ΔT_U) from a given temperature occurs at a lower temperature than upon demagnetization (ΔT_D) from the same temperature. This difference is important for analysis of the cooling power of an AMRR as indicated by the cooling power equation given above.

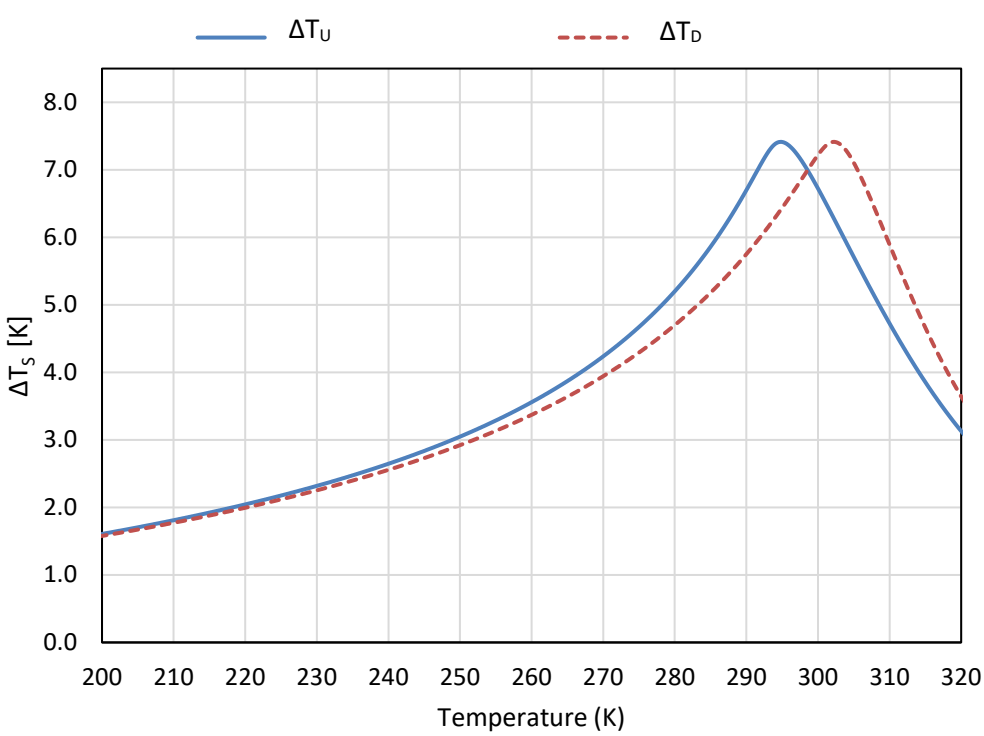

Figure 1. Adiabatic temperature changes (ΔT_S) for Gd upon magnetization from 0.6 T to 3.3 T (solid blue line) and upon demagnetization from 3.3 T to 0.6 T (dashed red line). The Curie temperature of Gd is ~293 K.

Propane Liquefaction Experiments

The pressures for the propane liquefaction experiments described in this paper were measured at the propane lecture bottle regulator as 52.0 psia for one experiment and 29.0 psia for the second experiment. The supply temperatures at the lecture bottle for these two experiments were measured as 295.7 K and 295.2 K, respectively. The average propane temperatures measured in the cold heat exchanger (CHEX) during liquefaction were 262.5 K and 246.0 K which give equilibrium pressures in the condensing heat exchanger of 49.0 psia and 27.2 psia, respectively. Data from Refprops for pure propane at different pressures show propane liquefies at 231.0 K at 0.1013 MPa (14.695 psia); at 246.0 K when the pressure is 27.2 psia, and at 262.5 K with the pressure at 49.0 psia. The small pressure drops for propane from the lecture bottle to the condensing heat exchanger is from flow through the 0.635 cm (¼") outer diameter feed tube ~2 m long from the lecture bottle into the AMRR. As soon as the initial propane is liquefied in the small storage tank, the large volume decrease upon condensation creates a cryopump that continuously draws the propane through the helium-cooled heat exchanger to create continuous thermal load until the small propane storage volume is full. These temperatures are easily within the capability of an experimental single-stage AMRR prototype successfully developed and characterized at PNNL using dual 1.05 kg Gd regenerators reciprocating in and out of a high-field superconducting magnet. Figure 2 illustrates the dual regenerators and the condensing heat exchanger used for this experiment.

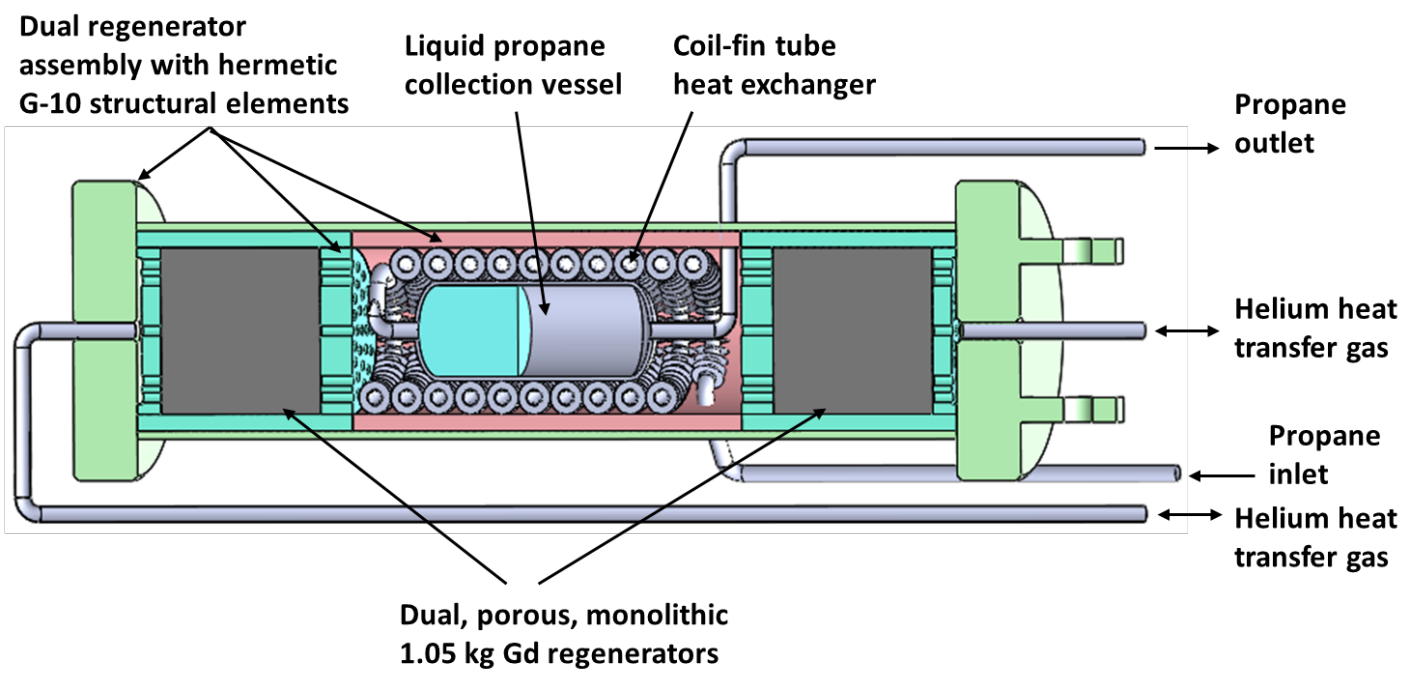

Figure 2. A schematic of the coiled-fin tube condensing HEX and propane storage vessel in the dual Gd regenerator and CHEX subsystem with heat transfer gas and propane connecting tubes. The identical reciprocating Gd regenerators have opposing axial hot-to-cold temperature profiles and alternatively produce cold helium flow through the condensing heat exchanger when one regenerator in high field and the other is in low field.

This apparatus[33] is capable of cooling from a hot temperature of ~285 K to ~218 K with no external thermal load, i.e., only continuous intrinsic parasitic heat leak of ~15 W at ~218 K. At a cold temperature of ~260 K, the

apparatus has an external cooling power of ~60 W in the CHEX at 0.25 Hz, with ~4 gm/s of 200 psia He gas during the blow steps of the AMR cycle, and 3.3 T to 0.6 T field change (the parasitic heat leak at this temperature is ~6 W). Given this operating range, this AMRR apparatus (also called GEN-I in figure 3) can liquefy propane at the two pressures chosen. The results will help validate predictive performance models and identify design issues for advanced designs of AMRR prototypes for liquefaction of colder cryogens such as LNG and LH_2.

Simple Piping & Instrumentation Diagram (P&ID) for propane liquefaction within dual regenerator-CHEX

Several simple modifications were made to existing apparatus to safely execute experiments to measure the temperatures, pressures, flow rates, and control during liquefaction of pure propane feedstock starting from near room temperature. A schematic of simplified P&ID of the modified dual-regenerator and CHEX subsystem in the apparatus to enable propane liquefaction is shown in Figure 3. Pure (99.5+ %) propane at 115 psia in a regulated lecture bottle filled with 454 grams was purchased. This mass of propane is sufficient for several experimental runs. The lecture bottle includes a pressure regulator and a manual flow-control valve. A 0.635 cm (¼") o.d. stainless-steel (ss) tube ~2 m long from the lecture bottle to the CHEX included a flexible ss section at the top of the central access ss insert tube in the AMRR apparatus. This hermetic tubing supplies propane at desired pressures into a compact ss coiled-fin tube heat exchanger with a small thin-wall ss cylindrical collecting vessel mounted inside the coil-fin tube heat exchanger. The heat exchanger and collecting vessel assembly was sized to fit into the ~5 1/2" long by 2.5" i.d. of the CHEX in place of the external-load heater assembly used in previous experiments. An Alicat pressure, temperature, and mass flow measuring instrument, additional ¼' tubing with a check valve, plus a pressure relief valve (PSV) set to 80 psia were installed on the vent line into a nearby fume hood which has a large enough continuous air suction rate to insure excellent dilution of the small amount of propane gas used in these experiments.

Configuration of AMRR Apparatus for Propane experiments

Cold heat exchanger assembly to condense, liquefy, and collect liquid propane

The compact propane heat exchanger was designed to liquefy the propane gas as it flows through a coiled fin tube and into a small collecting vessel located within the CHEX. The coiled-fin-tube heat exchanger was designed to remove 38 W of heat from the propane process stream and achieve a final temperature of 264 K at a pressure of 52 psia. It was sized to account for the heat transfer coefficients of both the helium heat transfer gas as it flows around the fins on the exterior of the helical heat exchanger tube and the propane flowing inside the heat exchanger tube. According to standard heat exchanger design calculations[34], the primary resistance to heat transfer is the propane gas during precooling (~12 $W/m^2/K$). Once propane begins to condense and produce a mixed phase, the primary heat-transfer resistance becomes ~200 psia helium flowing past the finned tubes external to the finned-tubes of the heat exchanger (255 $W/m^2/K$). These heat transfer design calculations were performed assuming fully-developed flow as the boundary condition. The transient behavior of the oscillatory helium gas flow during the hot-to-cold blow steps of the AMRR improves the heat transfer and provides design margin.

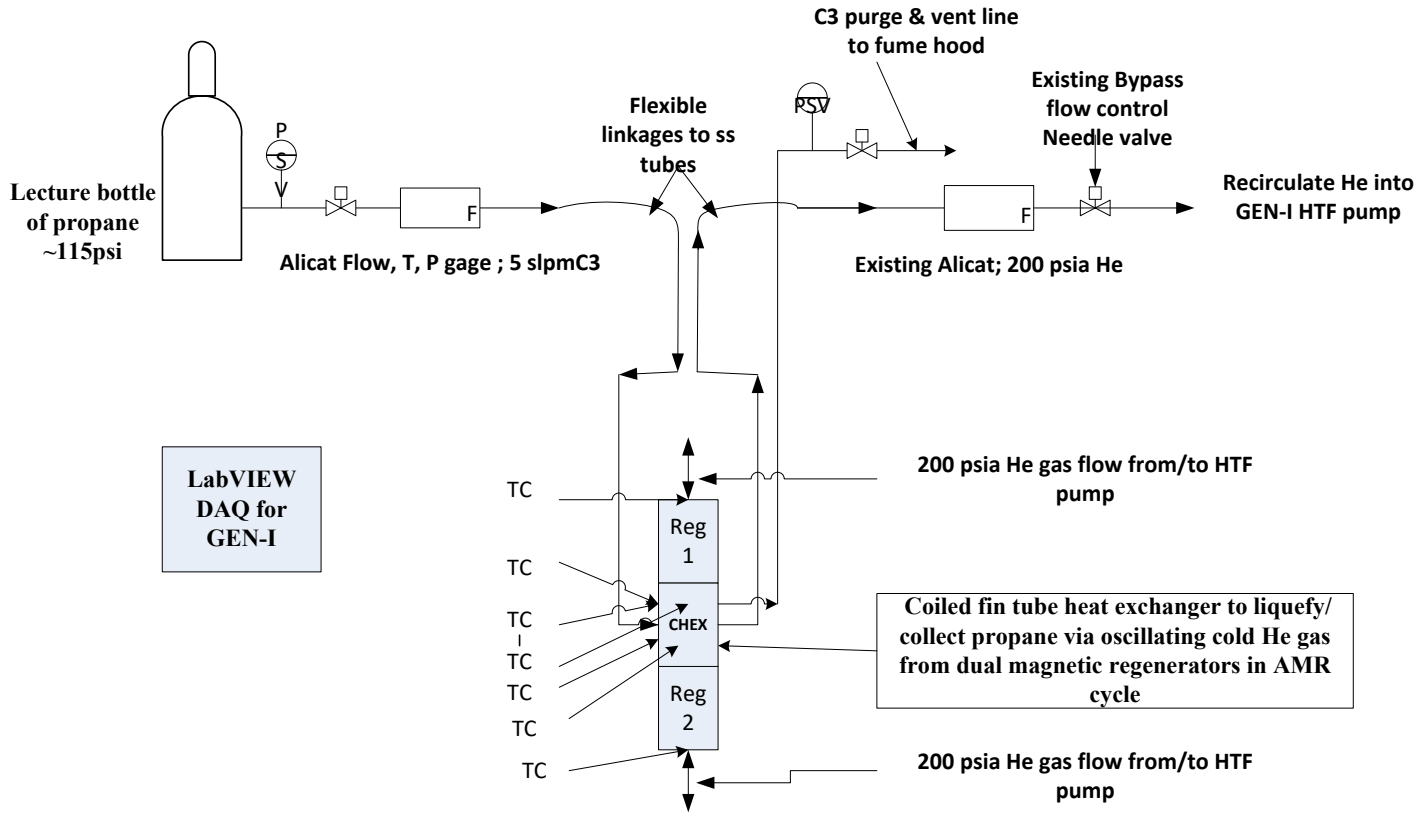

Figure 3 A simple process flow schematic of the AMRR apparatus subsystem with additional components required for propane liquefaction experiments. TC label indicates thermocouple locations.

The coiled, finned-tube HEX purchased from Energy Transfer MDE[35] is shown in Figure 4. The tube and fins were 304 stainless steel. The effective axial (z) length of eleven close-fitting loops of heat exchanger tubes is 14-cm (5-1/2”). Each loop is a length of ~16 cm (~6.3”) of 0.63 cm (¼”) diameter tube with 0.32 cm (1/8”) high regularly-spaced fins that are 0.05 cm thick (0.02”) brazed onto the tube surface. The ~180-cm long helical finned-tube is gradually bent into a circular coil, so the exterior fins of each tube fit snuggly inside the 6.35 cm (2.5”) inner diameter G-10 tube of the CHEX and the interior fins of each tube fit snuggly around the 3.8 cm (1.5”) diameter stainless-steel collection vessel. This configuration results in 11 close-fitting coils. The helium heat transfer gas in the AMRR apparatus is forced to flow through the fins on the coils, resulting in very effective heat transfer between the cold helium gas and the propane gas. The helium gas pressure drop through these fins in the CHEX is calculated to be less than 8 Pa. The internal volume of the coiled, finned-tube HEX is 27.04 cm^3 and it has a mass of 420 grams.

The propane collection vessel was constructed of a 3” long, 0.065” wall, 316 stainless steel tube section with butt-welded endcaps. The outer diameter of the welded tube was turned down 0.015” to form a tight fit into the center of the coil-finned tube heat exchanger. Small 0.125” diameter holes were drilled into both endcaps and 0.125” 316 stainless tubes were TIG-welded to each. The bottom tubing was welded to the outlet of the HEX while the top tube was welded to the propane vent line. The welded assembly is shown in Figure 4. The volume of the central collecting and storage vessel is 94.39 cm^3. Total liquid propane volume is 121.43 cm^3 due to the additional volume of the coiled tubes of the coil-finned tube heat exchanger. The connecting tubing from the coil-finned tube heat exchanger to the storage vessel plus the vessel has a mass of 190 grams. The propane liquefaction coil-finned tube heat exchanger was held in place within the CHEX with two machined G-10 endcaps

that were epoxy-bonded to both ends of the CHEX tube. The complete assemble with the Gd regenerator is shown in Figure 4.

To monitor temperatures of the inlet and condensed propane and helium heat transfer gas, four bare-tipped, 36-gauge, tightly-twisted type-E thermocouples coated with thin Teflon insulation were inserted through the G-10 outer tube wall of the CHEX and sealed with epoxy. Two thermocouples were dipped into dilute epoxy and cured to provide a very thin layer of insulation before being attached with epoxy to the entrance and exit of the condensing heat exchanger; the exit is near the bottom of the central liquid propane collector vessel in the assembly shown in Figure 4. The other two bare-tipped thermocouples were mounted in the helium gas flow path near the bottom and top of the liquid collector vessel shown in Figure 4 (and schematically in Figure 4).

Figure 4. A picture from the top of the compact coiled-fin tub g heat exchanger and liquid propane collection vessel. The dimensions of this assembly are in the text.

A LabVIEW-based data acquisition system (DAQ) was used to control the actuators and monitor all sensors. The actuators were controlled via serial communications and the sensors were read using National Instruments compact-DAQ cards. The DAQ program for the AMRR apparatus recorded the propane pressure, temperature, and flow meter and additional temperature measurements from thermocouples in the CHEX. The total amount of liquefied propane produced was measured with the flow-integration feature of the Alicat sensor for the two different runs. The large data files from these experiments were stored in Excel and later transferred to Origin for processing and plotting prior to analysis.

Prior to beginning experiments, the entire propane-containing assembly shown in Figures 2 and 3 was filled with nitrogen to ~60 psia and vented to ~16 psia. Then the assembly was filled with propane to ~60 psia and vented to ~16 psia into the fume hood. The propane filling and venting procedure was repeated several times to reduce any oxygen concentration within the propane liquefaction subsystem to well below lower flammable limits of any potential mixtures. After that step, the propane subsystem was pressurized to the desired feed pressure using the regulator on the lecture bottle of propane with the supply valve open to the condensing heat exchanger.

The AMRR apparatus was prepared for magnetocaloric cooling by charging the conduction-cooled magnet at 4 K to 3.3 T and putting it into persistent mode with the stationary dual Gd regenerators at the mid-point of the drive-actuator stroke. The dual chillers in the heat transfer fluid (HTF) subsystem were adjusted to give flowing helium gas temperature of ~285 K alternatively into the hot end of the demagnetized dual regenerator during the hot-to-cold blow step in the AMR cycle. Before the regenerator-drive actuator was started helium gas at ~200 psia from the HTF subsystem was driven back and forth for several minutes to establish a uniform initial temperature of ~285 K throughout the regenerators and CHEX subsystem.

Propane Liquefaction Experimental Results

In the first experiment, the propane pressure regulator was adjusted to fill the propane assembly to ~52 psia as measured the pre-calibrated Alicat mass flow meter near the propane lecture bottle that also measured the propane supply temperature, pressure, and total accumulated mass flow. The propane feed gas temperature of 295.7 K was measured at the Alicat sensor located near the lecture bottle. The propane flow control valve on the lecture bottle was kept open with zero flow as expected when the entire process gas system is filled at stable equilibrium conditions and the PSV is set at 80 psia. The drive actuator was started to immediately produce cooling from the Gd executing the AMR cycle at 0.25 Hz with equal time steps for each step of the AMR cycle with 200 psia helium gas flowing at ~4 gram/sec in the HFT hermetic assembly. The temperatures at the top (propane inlet) and bottom of the coil-fin tube HEX where it connects to the small storage vessel began to immediately decrease with no measurable flow of propane (the control valve on the lecture bottle was not adjusted during the entire run). As shown in Figure 5 the propane flow rate measured at the lecture bottle increased rapidly when the CHEX reached ~262.5 K but rather quickly decreased to an approximately constant value with a gradual decrease until a sudden drop to zero near the end of the run. Although the propane pressure was set by the regulator at the lecture bottle, the propane flow rate was determined by the helium gas cold temperature in the CHEX and cryopumping caused by propane condensation in the coiled-fin tube heat exchanger. After ~200 seconds the initial high flow rate drops by about a factor of two. Propane liquefaction continued at an approximately constant accumulation rate for ~1500 seconds. An average propane flow rate was calculated by dividing the total collected mass of liquefied propane by the total elapsed time of liquefaction.

Accumulated propane flow as a function of time steadily rose from zero in the first experiment as shown in Figure 6. Figure 6 also shows T_{COLD} of He gas in the CHEX is approximately equal to that in the coiled-fin tube heat exchanger and stabilized at 262.5 K for several minutes of liquefaction before the propane collection vessel temperature slowly decreased indicating collected propane was being subcooled. Sub-cooling continued until T_{COLD} reached ~245 K and the propane supply flow-rate dropped to zero and accumulated liquid propane volume

was constant. At this time, the rate of sub-cooling noticeably increased and the whole CHEX assembly eventually approached steady-state at ~218 K after about an hour as in previous experiments in this AMRR apparatus under these operating conditions (i.e., with the only thermal load from parasitic heat leak).

In a second experiment, the propane supply pressure was reduced to 29.0 psia and everything was prepared in the same manner as in first experiment. This time the average CHEX cold temperature dropped to ~246 K before propane started to flow from the lecture bottle and liquid propane accumulated in the collection vessel. These data were recorded with the DAQ as before. The plotted temperatures at the inlet and exit of the coiled-fin tube heat exchanger and the accumulated volume of propane vs. time from the DAQ file for the second experiment are shown in in Figure 7. In the second experiment propane liquefaction began at an average temperature of 246 K which is the equilibrium temperature of liquid propane at 27.2 psia. Liquefaction continued at an approximately constant accumulation rate for 2240 seconds with the collected liquid propane subcooling as in the first experiment.

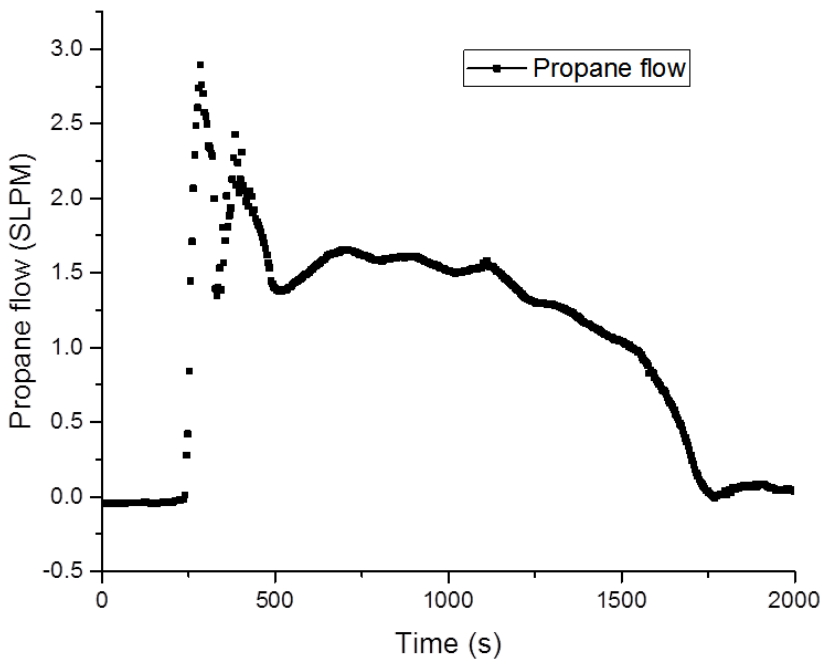

Figure 5. The instantaneous propane flow rate in standard liters per minute as a function of time during the liquefaction run at 52.0 psia. Note the time scale in this figure is different from that in Figure 6.

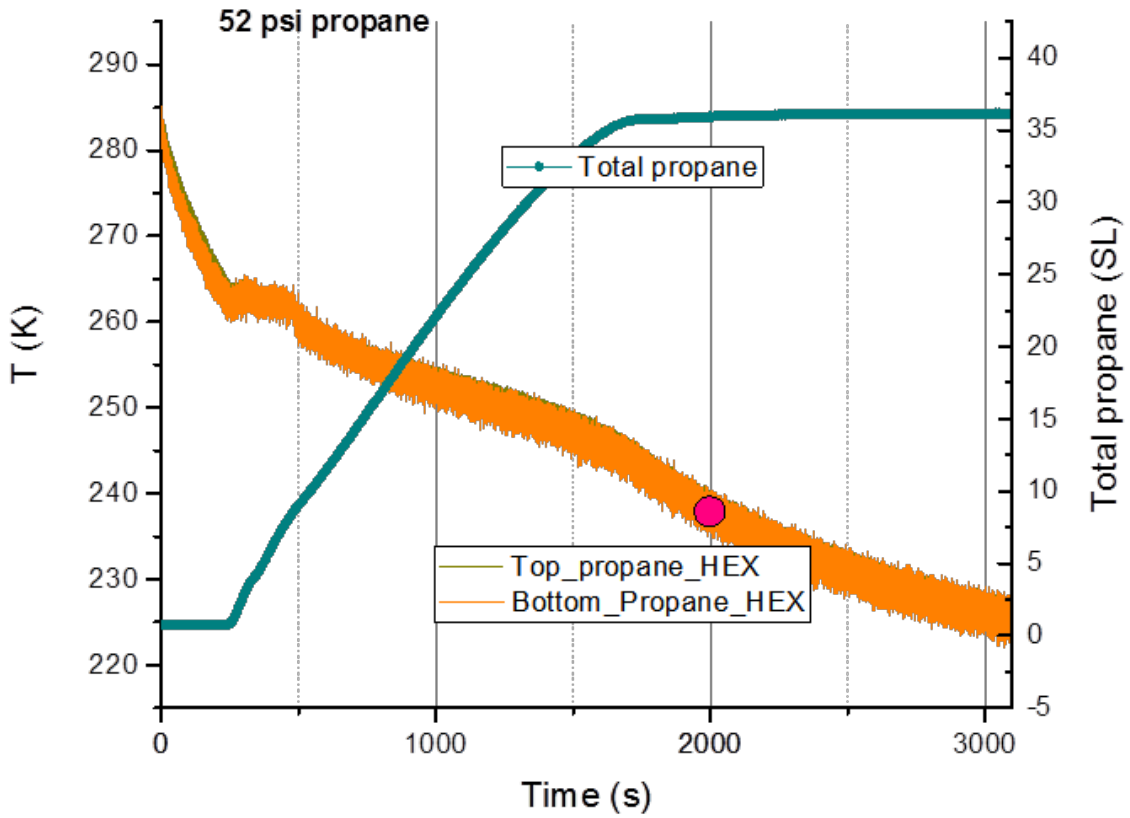

Figure 6. Temperatures on the coiled-fin tube heat exchanger and collection vessel and total volume of propane as a function of time for propane liquefaction in the first experiment (52.0 psia feed pressure at lecture bottle). The red dot is where temperature vs. time data were expanded (not shown) over 3-4 cycles for analysis of Gd cooling power from cool-down rate.

After approximately steady-state conditions were reached at the end of the experiments, the regenerator drive actuator was stopped. The vent valve that bypassed the PSV was slowly opened enough to reduce the propane-storage vessel pressure to ~16-20 psia as the CHEX gradually warmed up toward ~285 K over about 2 hours.

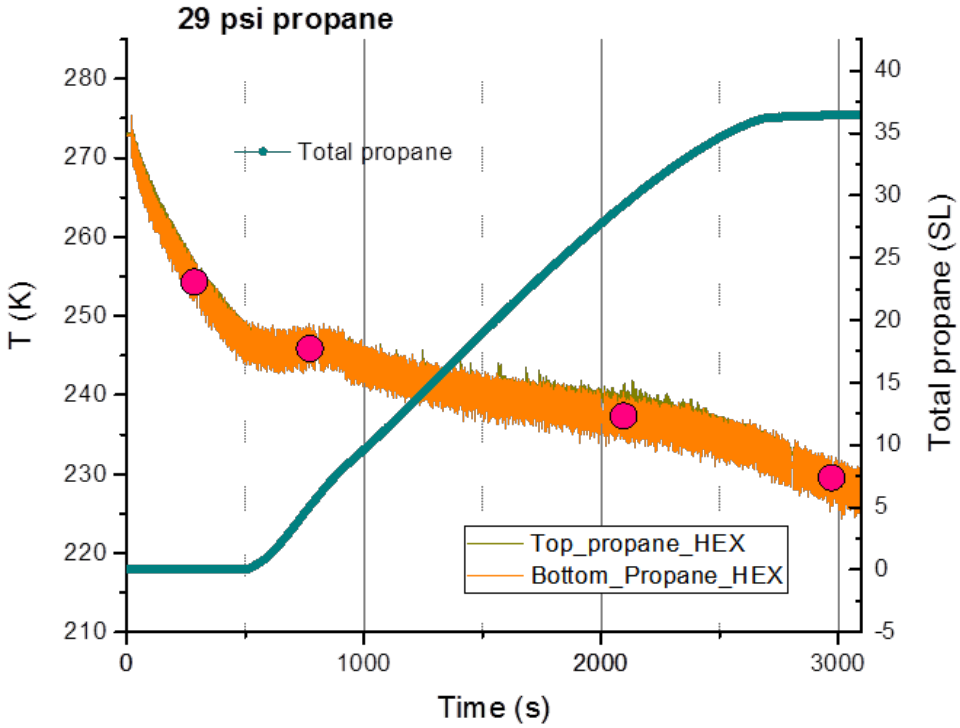

Figure 7. Temperature on the coiled-fin tube HEX and total propane as a function of time for propane liquefaction in the second experiment (29.0 psia feed pressure at the lecture bottle). The red dots were places where the temperature vs. time plotted data were expanded (not shown) over 3-4 cycles.

Analysis of propane liquefaction experiments

Cool-down curve analysis

The cooling power can also be calculated from the rate of cool down (K/s) of the estimated thermal mass of the CHEX, the propane liquefaction HEX/storage vessel, and colder sections of the dual regenerators on the initial steep section of the T vs. time curve in Figure 6. This calculated value of cooling power is 64.3 W; it already includes the parasitic heat leaks external to the regenerators from radiation and conduction to the moving air during the reciprocating motion of the regenerator assembly. Similarly, in the first experiment the red dot located at 233.5 K in Fig. 6, the total Gd cooling power from the cool-down rate (including additional thermal mass of 65 grams of liquid propane) is 33.4 W. Similar analyses of the measured data were repeated for the data at corresponding red dots in Figure 7. The cooling power of the Gd regenerators only occurs during the 1-second cold helium flows in the hot-to-cold flow steps of the AMR cycle, i.e., only ½ of the 4-second period. These cooling-power results for the AMRR apparatus under the given operating conditions are plotted in Figure 8. A linear least-square fit was drawn through these points for illustration.

Propane liquefaction data analysis

A large amount of information was obtained by analysis of the experimental data. In the first experiment, the total propane liquefied was ~36.0 standard liters and in the second experiment the total propane liquefied was ~36.5 standard liters. These values are consistent because there should be a slightly higher total propane mass in the second experiment than in the first experiment because the density of colder liquid propane in the second experiment is slightly larger than that in the first experiment. The Alicat mass flow meter at the lecture bottle was factory-calibrated for propane with flow rate in SLPM (standard liters per minute) and total flow in SL (standard liters) at standard conditions of 298.16 K and 14.695 psia. Using Refprops the density of pure propane

at the Alicat factory standard conditions is 1.832 kg/m3 which enables conversion of SLPM to kg/s and SL to kg of propane. The mass of liquid propane produced in the first experiment was 65.9 grams and the mass of liquid propane produced in the second experiment was 68.4 grams. As expected, the ratio of these values is close to the ratio of the densities of liquid propane at 262.5 K and 246 K. This agreement confirmed liquid propane is only produced in the coils of the HEX and enclosed collection vessel cooled to or below the dew point temperature of propane at the selected pressures.

The average rate of propane liquefaction from the data in first experiment is 4.40 x 10-5 kg/s. Multiplying this value times the measured total liquefaction time and dividing by density of propane at 262.5 K gives total liquid volume of 121 cm^3. Likewise, the same calculation for data from the second experiment gives an average liquefaction mass flow rate of 2.98 x 10-5 kg/s and a volume of propane of 121 cm^3. These volumes are in exact agreement with the combined volumes of the coiled-fin tube heat exchanger and the small collection vessel shown in Fig. 4 above. This result is expected because these two containers are the only process stream elements that are cooled by the cold helium gas. As soon as they fill up, the cryopumping pressure-difference from condensation of propane goes to zero and flow of propane from the lecture bottle stops.

The enthalpy difference between liquid propane at 262.5 K and 49.0 psia and gaseous propane at 295.66 K and 52.0 psia for the first experiment was calculated using Refprops (there was no pre-cooling of the propane gas but there was a small pressure drop in the tubing). The change in propane enthalpy between these state points times 4.40 x 10^{-5} kg/s gives an average cooling power during liquefaction of 19.6 W. In addition to the sensible and latent heats of liquefaction, Figure 6 shows that during the last 1213 seconds of the first experiment, the liquid propane was slowly subcooled from 262.5 K to 246.0 K. The average heat capacity of liquid propane at 49.0 psia over this sub-cooling temperature span divided by the elapsed time for associated sub-cooling requires an additional cooling power of 2.1 W for the first experiment. The sum of these two thermal loads requires 21.7 W of total cooling power for propane liquefaction. The thermal load from the propane liquefaction and subcooling into the CHEX control volume are continuous during the 4-second AMR cycle. The parasitic heat leaks also are continuous into the CHEX control volume. However, cooling from the dual Gd regenerators occurs every other second, i.e. half of the period of the AMR cycle. Therefore, to represent the net cooling power of the AMRR for the propane liquefaction and parasitic heat leaks on the same plot as the cooling power obtained from cool-down temperature vs. time data, the propane load and parasitic heat leak thermal loads must be doubled. This result is plotted as a green star in Figure 8 at 262.5 K.

For the second experiment, the enthalpy difference between liquid propane at 246.0 K and 27.2 psia and gaseous propane at 295.16 K and 29.0 psia was calculated using Refprops. This difference times the average mass flow rate 2.97 x 10^{-5} kg/s gives a cooling power of 14.5 W. In addition to the latent heat of liquefaction, during the last 1780 seconds of the second experiment the liquid propane was slowly subcooled as can be seen in Figure 7. The heat capacity of liquid propane at 27.2 psia was obtained from Refprops and averaged over the sub-cooling span from 246.0 K to 233.0 K (c.f. the experimental data) divided by the elapsed time for sub-cooling to give an additional required cooling power of 1.1 W for the second experiment. The sum of these two values gave total external thermal load from the propane liquefaction as 15.6 W. Using the same data treatment as described for the first propane liquefaction experiment, the cooling power of the AMRR apparatus for this experiment is plotted as a green star at 246 K in Figure 8. The agreement of the results from propane liquefaction cooling and cool-down cooling is very good.

Eddy Current calculations

Eddy currents are induced in each closed conducting loop from the magnetic induction changes during the AMR cycle within the stainless-steel finned tubes in the propane cooling and condensing heat exchanger shown in Figure 3. Each of the coiled fin tubes are in electrical contact with the thin-walled stainless steel propane collection vessel also shown in Figure 3. Calculating the emf caused by the magnetic flux changes, the resistance

of each loop and that of the storage vessel using known dimensions and resistivity properties, gives the eddy current thermal load into the CHEX of ~134 mW for 3.3 T to 0.6 T magnetic induction changes in 1 second twice per AMR cycle. This thermal load is negligible compared to the ~40-60 W of cooling power of the AMRR.

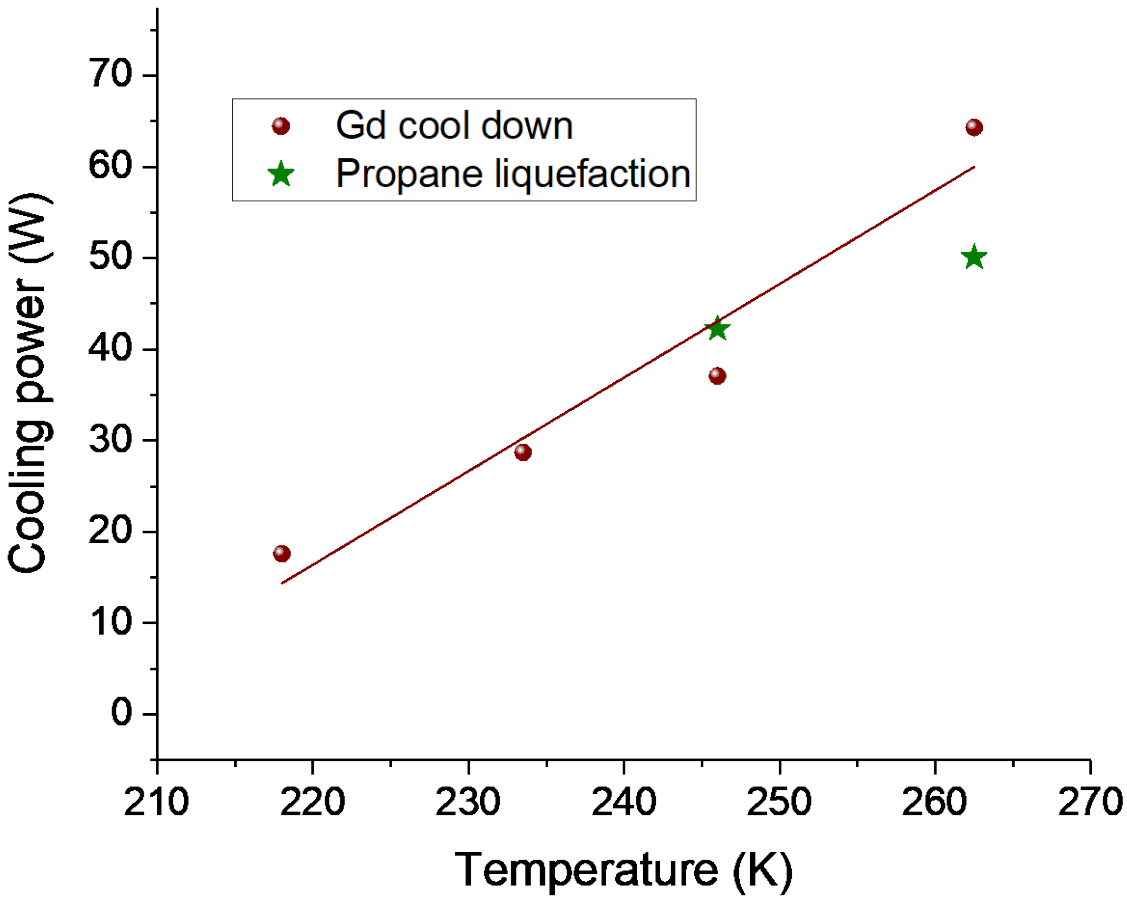

Figure 8. Several data points showing the cooling power from the dual Gd regenerators in AMRR apparatus obtained from the rate of cooling of the CHEX and regenerators given by cool-down temperatures vs. time at specific average cold temperatures are shown in this plot of thermal load vs. temperature. The cooling power of the AMRR apparatus for propane liquefaction are added as green stars.

The Biot numbers for the ss coiled-fin tube heat exchanger and the G-10 walls of the CHEX were calculated at 246 K and 262.5 K. As stated above, the calculated helium gas conductance to the coiled fin tube heat exchanger was 215 W/m^{2}K. The various temperature, pressure, and flow-dependent parameters for He, G-10, and stainless steel were calculated or obtained from the literature to give Biot numbers of 0.18 and 0.16 for the G-10 walls in CHEX at 246 K and 262.5 K, respectively. The Biot numbers for the ss process heat exchanger are 0.025 and 0.024 at 246 K and 262.5 K, respectively. These values suggest that a portion of the G-10 surfaces in the CHEX contribute to the thermal mass for the helium heat transfer gas in contrast to the thin walls of the stainless-steel components in the propane heat exchanger. This is consistent with the T vs. time curves.

Discussion

These experiments confirm our hypothesis that the coiled-fin tube heat exchanger and central storage vessel become a cryopump as soon as they are cooled by cold helium gas from the dual Gd regenerators to the condensation temperature of propane at a selected pressure. The cryopump action draws propane from the lecture bottle until the cooled heat exchanger and collection vessel are filled and the pressure differential due to propane condensation drops to zero, stopping the cryopumping, and no further liquefaction occurs. This is exactly what was observed in both experiments. Based on the relatively steady accumulated mass flow rate observed in both experiments, the flow caused by the cryopump action is continuous (at least compared to the DAQ data rate which is typically 0.1 second or less) and does not follow the intermittent cooling (every 2 seconds) of the dual regenerators in this reciprocating AMRR operating conditions. This result shows that thermal time constant of the condensation of propane is driven by the cold thermal mass of the heat exchanger, the collection vessel, and the liquefied propane much more than by the flow of cold helium gas in the CHEX. This observation also confirms that the process gas flow rate through process heat exchangers in a cryogenic liquefier with external process heat exchangers is not controlled by an inlet valve, but instead is controlled by the cooling power at the dew point temperature of the process gas at the pressure at the heat exchanger. This is commonly known in small-scale LNG liquefaction plants, but it is well reinforced herein.

In the propane liquefaction experiments, measurement of temperatures in the CHEX and liquefier process heat exchanger vs. time provide a good indication of the changing thermal loads from the propane and cool-down of thermal mass in the CHEX and process heat exchanger. For instance, as soon as the dew temperature of the propane is reached for the selected propane pressure, the rate of temperature decreases substantially which shows the latent heat from propane liquefaction is much larger than the sensible heat from gradually cooling the thermal masses in the CHEX/process heat exchanger which increases the applied thermal load to the cold helium gas flowing in the CHEX. The propane cool-down temperature curve changes again once liquid propane accumulates in the collection vessel and again when propane liquefaction ceases. The temperature continues to drop as the sensible heat of all the cold parts of the CHEX and the liquid propane are cooled to ~218 K which is the ultimate cold temperature limit of the AMRR at these operating conditions from the parasitic heat leak. This measured parasitic heat leak of ~17 W is consistent with calculated parasitic heat leaks from radiation, convection, and conduction mechanisms in the AMRR apparatus.

Another observation from Figures 6 and 7 is that the rate of accumulated propane mass during liquefaction is approximately constant during the entire liquefaction time span. At first glance, this is puzzling given cooling from the dual Gd regenerators occurs during hot-to-cold blows of helium gas from the demagnetized regenerator into the CHEX every other second during an AMR cycle. However, considering a control volume around the CHEX with heat flows into it [or out of it], allows proper allowance for intermittent and continuous heat flows. This situation also occurs when an external thermal load from a continuous heater in the CHEX is used to determine the load curve of the AMRR apparatus.

Conclusions

The use of an AMRR to successfully liquefy propane has been demonstrated. The excellent agreement between predicted and observed results confirmed our understanding of the design. Futher, the intermittent cooling of a reciprocating dual regenerator design was proven important for future reciprocating dual regenerator liquefier designs. The results of this work motivated the conceptualization of a new liquefier design using two sets of identical reciprocating dual-regenerator AMRRs with their drive actuators phased 90 degrees apart coupled with heat transfer gas flows distributed properly with several 3-way valves to direct the cold helium heat transfer gas in counterflow with the process gas can provide continuous cooling of the process gas. Such a design for liquid

hydrogen would require four multi-material magnetic regenerators and two superconducting magnets for a ~280 K to ~120 K high-FOM stage and another four multi-material magnetic regenerators and two superconducting magnets for a ~120 K to ~20 K high-FOM stage. This conclusion suggests using a continuously rotating wheel-type AMRR configuration with regenerators attached to the rim may be a much simpler alternative if the rotary seals and magnet configuration issues can be resolved.

Acknowledgements

It is a pleasure to acknowledge the financial and programmatic support of the Fuel Cell Technology Office of the Energy Efficiency and Renewable Energy Office of the Department of Energy. The pro-active support of DOE program managers Dr. Erika Gupta and Dr. Neha Rustagi is deeply appreciated. The help of numerous supporting staff at PNNL is also appreciated. Dr. John Barclay appreciates the opportunity for EENW to participate in the MCHL project at PNNL.

References

[1] J.R. van Geuns; Doctoral Thesis; Univ. of Leiden, (1966); "A Study of a New Magnetic Refrigeration Cycle"

[2] Y. Hakuraku and H. Ogata, J. Appl. Phys. 60, 3266 (1986) "A rotary magnetic refrigerator for superfluid helium production".

[3] H. Nakagome et al., Adv. Cryog. Eng. 29, 581-587 (1984). "The helium magnetic refrigerator: I – Design"

[4] T. Numazawa et al., Adv. Cryog. Eng. 29, 589-596 (1984); "The helium magnetic refrigerator: II – liquefaction process and efficiency"

[5] G. V. Brown, J. Appl. Phys, (1976), 47, 3673-80 "Magnetic heat pumping near room temperature"

[6] W. A. Steyert, Jr., J. Appl. Phys. (1978) 49 1216 "Stirling-cycle rotating magnetic refrigerator and heat pump for use near room temperature:

[7] J. A. Barclay and W. A. Steyert, Jr., U.S. Patent 4,332,135; June 1, 1982, "Active Magnetic Regenerator"

[8] J. A. Barclay, The theory of an active magnetic regenerative refrigerator, in: "Proc. of the 2nd Biennial Conf. on Refrigeration for Cryogenic Sensors and Electronic Systems," NASA Goddard Space Flight Center, Greenbelt, MD (1982).

[9] Astronautics Corporation of America, Final Report to DOE on Contract No. DE-AC02-90CE40895 compiled by D. J. Janda, chief project engineer, (July 2, 1992), "Magnetic Liquefaction of Hydrogen".

[10] J.A. Barclay and T.C. Brook; U.S. Patent 6,467,274 B2; October 22, 2002; "Apparatus and Methods for Cooling and Liquefying a Fluid using Magnetic Refrigeration".

[11] K. Oseen-Senda, M. P. Skrzypkowski, and J.A. Barclay; SBIR Phase I Final Report (2008); "Active Magnetic Regenerative Hydrogen Liquefier"; Contract No. DOE SBIR DE-FG02-07ER84783

[12] A. Rowe and A. Tura; Int'l. J. of Refrig.; 29, 1286-93 (2006); Experimental investigation of a three-material layered active magnetic regenerator".

[13] A. Rowe, Cryogenics, 52, 111-118 (2912) "Thermodynamics of active magnetic regenerators: Part I"

[14] A. Rowe; Cryogenics 52, 119-128 (2012) "Thermodynamics of active magnetic regenerators: Part II"

[15] A. Smaili and R. Chahine; Cryogenics 38, 247-252 (1998) "Thermodynamic investigations on optimum active magnetic regenerators"

[16] T. Utaki et al.; Cryocoolers 14, 645 (2007) "Research on a Magnetic Refrigeration Cycle for Hydrogen Liquefaction"

[17] K. Matsumoto et al.; Cryogenics, 51, 353 (2014) "Numerical Analysis of AMRs for hydrogen magnetic refrigerators between 20 K and 77 K"

[18] T. Numazawa et al.; Cryogenics 62, 185, (2014); Magnetic refrigerator for hydrogen liquefaction"; and several references herein.

[19] Y. Kim, I. Park, and S. Jeong; Cryogenics, 57, 113 (2013), "Experimental investigation of two-stage active magnetic regenerative refrigerator operating between 77 K and 20 K".

[20] I. Park and S. Jeong, Cryogenics, 88, 106 (2017); "Development of the active magnetic regenerative refrigerator operating between 77 K and 20 K with the conduction cooled high-temperature superconducting magnet"

[21] B. Yu et al., Int'l J of Refrigeration, (2010), 33, 1029-1060 "A Review of Magnetic Refrigerator and Heat Pump Prototypes built before the year 2010".

[22] C. Zimm, et al., (1998), Adv. Cryog. Eng. (1998), 43, 1759-1766 "Description and performance of a near room temperature magnetic refrigerator"

[23] J. A. Barclay, K. Oseen-Senda, L. Ferguson, A. Cousins, J. Pouresfandiary, H. Ralph, T. Hampton; Final tech Report: DOE Contract

Number DE-FG36-08GO18064; (2014) “Active Magnetic Regenerative Liquefier for Hydrogen”
[24] J. Holladay, K. Meinhardt, E. Polikarpov, E. Thomsen, J. Barclay, J. Cui, I. Anderson, B. Jensen; MagnetoCaloric Hydrogen Liquefaction”; DOE Annual Merit Review, PD131 (2017), Tech report.
[25] J. Holladay, R. Teyber, K. Meinhardt, E. Polikarpov, E. Thomsen, C. Archipley, J. Barclay; accepted for publication in Cryogenics, (2018); “Investigation of Bypass Fluid Flow in an Active Magnetic Regenerative Liquefier”
[26] J. A. Barclay, K. Oseen-Senda, M. P. Skrzypkowski, Int’l Institute of Refrig.; Proc of Thermag VI, Victoria, B.C. 7-10 September 2014; “Unique Features of Liquefaction of Hydrogen and Natural Gas using Magnetic Refrigeration”
[27] R. Teyber, K. Meinhardt, E. Polikarpov, E. Thomsen, J. Holladay, J. Cui, and J. Barclay; submitted to Applied Energy; July 22, 2018; "Performance investigation of a high-field active magnetic regenerator"
[28] R. F. Barron; Cryogenic Systems; 2nd ed., Oxford University Press, NY (1985)
[29] See reference 7
[30] See references 23 and 11 for more details of numerical model.
[31] A. Tishin, K. Gschneidner, Jr., V. Pecharsky; Phys. Rev. B; 59, (1999) 503-511; “Magnetocaloric effect and heat capacity in the phase-transition region”
[32] S. Dan’kov, A. Tishin, V. Pecharsky, K. Gschneidner, Jr..; Phys. Rev. 57B, (1998) 3478-3490; “Magnetic phase transitions and the magnetothermal properties of gadolinium”.
[33] See references 23 and 24 for more details of this active magnetic regenerative refrigerator prototype.
[34] See reference 27 for example.
[35] https://www.finnedtube.com